Final Manuscript

Fire detection using smoke and gas sensors

Shin-Juh Chen[1], Chris Hovde[1], Kristen A. Peterson[1], and André Marshall[2]

[1] *Southwest Sciences Inc., 1570 Pacheco Street, Suite E-11*
Santa Fe, NM 87505, USA
[2] *Department of Fire Protection Engineering*
University of Maryland, College Park, MD 20742-3031, USA

Submitted to
Fire Safety Journal

Paper No. 1298
Manuscript No. U161

January 17, 2007 (2:07pm)

Corresponding Author:
Shin-Juh Chen, Ph.D.
Southwest Sciences, Inc.
1570 Pacheco Street, Suite E-11
Santa Fe, NM 87505

TEL: (505) 984-1322
FAX: (505) 988-9230
EMAIL: sjchen@swsciences.com

TABLE OF CONTENTS

Fire detection using smoke and gas sensors

Shin-Juh Chen[1], Chris Hovde[1], Kristen A. Peterson[1], and André Marshall[2]

[1] *Southwest Sciences Inc., Santa Fe, NM 87505, USA*
[2] *Department of Fire Protection Engineering*
University of Maryland, College Park, MD 20742-3031, USA

Abstract

Fire detection systems located in aircraft cargo compartments are currently based only on smoke detectors. They generate about 200 false alarms per year for U.S. registered aircraft. The number of false alarms is growing as more planes are outfitted with smoke detectors and air travel expands. Moreover, the survivability of an aircraft in a fire scenario depends on the early detection of the fire. A fire detection system is developed based on the simultaneous measurements of carbon monoxide, carbon dioxide, and smoke. The combination of the rates of rise of smoke and either carbon monoxide or carbon dioxide concentration provides a potential fire alarm algorithm to increase the reliability of aircraft smoke detectors, and to reduce the time to alarm. The fire detection system with the alarm algorithm detected fires that were not alarmed by smoke sensors, and alarmed in shorter times than smoke sensors operating alone.

Keywords: fire detection, gas sensor, smoke, carbon monoxide, carbon dioxide, rate of rise, alarm algorithm, nuisance sources, fire signatures, aircraft cargo

1. Introduction

Fire detection systems of current aircraft cargo compartments are primarily smoke detectors. Existing smoke detectors have never failed to indicate an *actual* fire onboard an aircraft. The false alarm rates, defined as the percentage of alarms with no verified smoke in the cargo compartment, are as high as 99 percent. The cost of a false alarm is estimated between $30,000 to $50,000 per incident [1]. Moreover, there are safety issues associated with false alarms. Unfortunately, the cause of a false alarm is usually not known. Regulations mandate that the alarm sounds within one minute after the onset of a fire condition. Pilots may have only about ten or fifteen minutes in which to land before smoke or damage to the structure from an uncontained fire prevents the pilot from controlling the aircraft. Reducing the time to alarm will allow the pilot to suppress the fire at an earlier stage and permit more time to land the aircraft safely.

Previous fire detection algorithms used data from sensors for temperature, smoke, and combustion products. Some of the chemical species included oxygen (O_2), carbon monoxide (CO), carbon dioxide (CO_2), water vapor (H_2O), hydrogen cyanide (HCN), acetylene (C_2H_2), and nitric oxide (NO). Simple fire alarm algorithms are based on thresholds for maximum values, rates of increase, and combinations thereof from multiple sensors. Alarm algorithms based on threshold values are highly sensitive to signal offsets (due to background concentration fluctuations or slow drift in calibration), demand measurements of high accuracy, and require accurate and frequent calibrations. To remedy some of these deficiencies, threshold values that adapt to the changing conditions of the environment were based on a comparison between the predicted and measured values in a time sliding window [2]. Rates of rise of CO_2 and CO have been used to identify flaming and non-flaming fires, and were compared to a

commercial smoke detector [3]. Fire alarm algorithms that use CO and smoke [4], and CO_2 and smoke [5] have shown reduction in nuisance alarms and response times. Ionization and photoelectric detectors, CO and CO_2 sensors using magnitude and slope information, and background subtraction were used to evaluate a fire alarm algorithm based on a probabilistic neural network [6]. Flaming fires were identified correctly, but smoldering fires were problematic. A fire detection system having a multi-criteria alarm algorithm and multi-component sensor system has the potential to reduce false alarms generated by individual fire detectors, and to reduce the time to alarm in the presence of fires.

A potential method to reduce or eliminate false alarms generated by aircraft smoke detector operating alone and to reduce the time to alarm is described here. The fire detection system combines the simultaneous measurements of smoke, carbon monoxide, and carbon dioxide. A simple fire alarm algorithm, based on the rates of increase of these three components, is developed and assessed using fire tests of combustible materials, liquid fuels, and nuisance sources.

2. Experimental Methods

Experimental data to test the fire alarm algorithm and compare its performance with a commercial aircraft smoke detector were obtained at the University of Maryland. Figure 1 shows the fire testing facility which is a 2.2-m high brick room with dimensions of 4 m × 1.4 m and is unventilated until each fire test is completed. Using a vacuum pump and a flow controller, combustion products are extracted from the ceiling and passed through a 3-m long tubing. The gases flow through the smoke detector, a 5-micron particle filter, and the gas measurement path. For each fire test, the gas sensing

system provides concentrations of CO and CO_2, and levels of smoke are reported using a commercial aircraft smoke detector.

The smoke detector, based on the method of light scattering, is used to measure smoke concentration which is reported in volt (V) once a second through an analog output. The factory setting for the smoke detector to alarm in a fire scenario is 5 V (threshold value) which corresponds to 15 percent per meter attenuation. The noise level, obtained from the experimental data, is 0.2 mV for an averaging time of 10 seconds. The smoke sensor alarms when the analog output signal exceeds or equal the threshold value. In the fire alarm algorithm described here, the output voltage signals are continuously recorded and the rates of increase are computed and used in the algorithm.

The detection of CO and CO_2 is accomplished using diode laser-based absorption spectroscopy and consisted of a laser module, InGaAs photodiodes, a gas measurement path, and a reference cell. The optical setup is shown in Fig. 2. The laser beam is split into two paths by a commercial fiber splitter: one fiber directs 90 percent of the light into the gas measurement path (*i.e.* a multiple pass cell) and unto an InGaAs photodiode detector; and, the other fiber sends 10 percent of the light through a 10-cm long reference cell, which contains pure CO at 15 kPa, and unto another InGaAs photodiode for self-checking the laser operation (*i.e.* line-locking). The Herriott-type multiple pass optics [7] is needed to obtain the required sensitivity of about 5 parts per million (ppm) for CO. The 20-m total optical path length is achieved with 32 laser spots in a circular pattern on each 5-cm dia. mirror, and the two mirrors are separated by 31.9 cm.

The laser module is a distributed feedback (DFB) diode laser that operates at a

nominal room temperature wavelength of 1565.5 nm. The laser is stabilized at 32°C using a thermoelectric cooler to access the CO and CO_2 absorption lines near 1566.6 nm. Figure 3 shows the computed spectra of these two gases based on the HITRAN database [8]. The two absorption lines are accessible by scanning (via laser current) only less than one wavenumber (i.e. 1 cm^{-1}), within the tunning range of a DFB laser, and overlap over a region that covers 1/3 cm^{-1}.

To improve the measurement sensitivity, standard wavelength modulation techniques [9,10] are implemented. The modulation frequency, *f*, is 250 kHz, and the demodulated signal at twice this frequency gives a line shape that resembles the second derivative of the direct absorption spectrum. Spectra are acquired by ramping the laser current at 1 kHz over one wavenumber and averaged for 1 second. Spectra of 50 ppm CO and 1 percent CO_2 were acquired initially to determine the appropriate least-square fitting basis functions. The concentration of CO and CO_2 in the measurement path is found by least-square fitting the measured 2*f* spectrum to a model that includes a quadratic background and the spectra of CO and CO_2, for a total of 5 fitted parameters. The pressure and temperature in the measurement path are needed as well for obtaining quantitative measurements.

3. Fire Alarm Algorithm

Candidate parameters for developing a suitable fire alarm algorithm include concentrations of major species (e.g. CO, CO_2), minor species (e.g. HCN, C_2H_2, NO) and smoke. Initial burn tests of toluene, heptane, methanol, newspapers, acrylic sheets, and wood were used to assess the potential of CO, CO_2, HCN and C_2H_2 as indicators of a fire event. Strong CO and CO_2 signatures were detected in smoldering and flaming

fires, respectively. Weak C_2H_2 signature was detected for a short time, and no HCN signature was detected by the instrument. Based on these measurements, only concentrations of CO, CO_2 and smoke are used a parameters in the fire alarm algorithm.

The algorithm in this paper uses the time derivatives of smoke levels, CO and CO_2 concentrations. Figure 4 illustrates the decision tree for this algorithm. Initially, the rate of increase of smoke level is checked continuously. If its rate of rise exceeds its predetermined threshold rate, then the SMOKE_Alarm parameter is set to 1; otherwise, the SMOKE_Alarm parameter remains 0. When the SMOKE_Alarm parameter is set to 1, the rates of rise of CO and CO_2 concentrations are then checked simultaneously. And, if either the rate of rise of CO or CO_2 concentration exceeds their corresponding predetermined threshold rate, then either CO_Alarm parameter is set to 1 or CO2_Alarm parameter is set to 1. When either CO_Alarm or CO2_Alarm parameter is set to 1, a fire alarm is initiated; otherwise, no fire alarm is set off and the next rate of increase of smoke level is computed and checked again. The performance of this fire alarm algorithm is compared to that of a smoke detector which alarms when its output signal exceeds a threshold value. The fire alarm algorithm described herein is *patented* [11].

4. Results and Discussions

4.1 Fire signatures of selected materials

A total of 30 fires, either smoldering or flaming, were generated to test the fire alarm algorithm described above. Combustible materials included samples of HDPE beads, PVC clad wire, mixed plastics, mixed fabric, and green canvas. Liquid fuels included methanol, heptane and toluene. The samples were ignited using different methods depending on the type of material. Liquid fuels were ignited using a lighter.

Other materials were ignited using a glowbar or a small pilot flame from a butane torch. Two to three burn tests were conducted for each material, and two methods of ignition were used for some of the materials. Table 1 shows the list of materials tested, the ignition method employed, and the type of fires generated.

Figures 5 – 7 show the time histories of CO, CO_2 and smoke concentrations, and the fire status for heptane, toluene, and HDPE beads, respectively. The figures of fire status are visual indications of the fire process with the numbers (0 – 4) denoting *unknown* (0), *igniting* (1), *smoldering* (2), *flaming* (3), and *not burning* (4). The fire status is useful in comparing the predicted and recorded times of the onset of smoldering or flaming fires to assess the responsiveness of the fire alarm algorithm.

The results of toluene and heptane show an immediate transition to a flaming fire after ignition. This is indicated in Figs. 5 and 6 where concentrations of CO, CO_2 and smoke begin to rise at the same time. On the other hand, the results of HDPE in Fig. 7 show a period of smoldering fire (indicated by a sharp rise in CO and smoke concentrations) immediately after ignition, then transitioning to a flaming fire 180 s later (indicated by a sharp rise in CO_2 concentrations).

Noise in the CO and CO_2 measurements were 3 and 600 ppm, respectively. As a result, the background concentrations of CO and CO_2 in the atmosphere prior to the burning tests cannot be measured. Noise and baseline drift can be minimized by selecting absorption lines of CO and CO_2 that do not overlap with each other. The limited tuning range of the DFB laser prevented the full resolution of these absorption line shapes. The use of a vertical cavity surface emitting laser, which can scan several absorption lines over a single laser current scan, could potentially resolve these issues. Additional calibration of the gas measurement system could reduce the baseline drift as

well.

4.2 Computing rates of increase

Two methods to compute the time derivatives of CO, CO_2, and smoke concentrations are used. The first method, denoted as *Method A*, performs a linear regression to provide a straight line fit to the raw data points for a given time history window. A time window of 10 seconds is chosen here to illustrate the following data processing scheme. When the data acquisition software is initially started, the first ten points are all new data. In subsequent times, the first nine points will be from previous times, and only the 10^{th} point is the new datum at the current time. The time derivative of this straight line fit is simply its slope and corresponds to the rate of increase of the corresponding parameter in the analysis. This is the simplest and most straight-forward method to implement with minimum computation and memory storage.

The second method, denoted as *Method B*, is to first perform a moving average on the raw data points within the prescribed time history window prior to performing the linear regression fit. For each data point within the time window, an average is computed using the data point of interest and its previous nine data points. This method smooths the fluctuations seen in the raw data. Figures 8a and 8b show CO and CO_2 time series data, respectively, for HDPE pellets smoothed using a time window between 1 and 20 seconds. For illustration purposes, each curve is shifted upward by 15 and 1000 ppm for CO and CO_2, respectively. This method works best when the natural background fluctuations of the chemical species are small. Using a long averaging time makes the sensor's white noise smaller, thus possibly permitting the use of much lower threshold rates than *Method A*. When the natural background fluctuations are resolved,

there is no advantage in using a longer time window, since the thresholds cannot be further reduced without causing false alarms. This method increases the required computation and memory storage as compared to *Method A*.

In addition, noise in the measurements contribute noise in the temporal derivatives of concentrations. Using a longer time history window reduces the scatter in the measured derivatives by $t^{3/2}$. However, it takes a longer time for the computed derivatives to reach the ideal slope of noiseless signal. In fact, for a smoke or gas signal that abruptly begins to increase with a constant slope, the time to reach the ideal slope value is given by the time window length. For the system to alarm reliably, the smoke and gas derivative signals should reach some multiple of the noise, for instance, five standard deviations. The time to alarm is then proportional to t^{-a}, where a is approximately between 5/10 and 6/10 as shown in Figs. 9a and 9b for CO and CO_2, respectively. The standard deviations were computed over the same time interval (180 s) for each of the time history window. The standard deviations are reduced sharply by more than 2.5 times as the time window is lengthened from 1 to 10 seconds.

The threshold rates of CO, CO_2, and smoke concentrations used in the fire alarm algorithm are obtained from the fire test results of heptane. For *Method A*, the threshold rates of increase for CO, CO_2 and smoke concentrations are 0.15 ppm/s, 25 ppm/s, and 1 mV/s, respectively. For *Method B*, the threshold rates of increase are 0.05 ppm/s and 8.0 ppm/s for CO, CO_2, and smoke concentrations, respectively.

4.3 Performance of three-component based fire alarm algorithm

Referring to Table 1, for each fire test, the time to the onset of visual smoke or fire, the time to alarm by the smoke detector, the time to alarm by the fire alarm algorithm

using *Method A*, and the time to alarm by the fire alarm algorithm using *Method B* are recorded. The times for observed onset of fires were recorded for all experiments. All reported times are referred to time equal zero when the data acquisition system starts collecting sensor signals. A time window of 10 seconds is used for the fire alarm algorithms.

Comparing fire alarm algorithms using Methods A and B, the times to alarm for the combustible materials do not differ considerably for both methods, except for the green canvas where it took 104 s longer for *Method B* to detect the presence of a fire. Both methods are suitable for implementation in a fire alarm algorithm.

The possibility of the smoke sensor to fail to alarm when operating alone (using a threshold method) is demonstrated by the four fire tests of heptane, methanol, PVC clad wire, and mixed fabrics. Because of low level of smoke present, the smoke sensor did not alarm in these tests. However, for the fire tests of toluene, HDPE beads, mixed plastics, mixed fabrics, and green canvas, the smoke sensor did alarm. The times to alarm by the smoke sensor can be as short as 9 s (toluene) and as long as 316 s (HDPE) when compared to the observed onset of the fires. The smoke sensor does not reliably and quickly detect the presence of fires when operating alone as a fire detection system.

The fire alarm algorithms using Methods A and B alarmed in cases where the smoke sensor did not even alarm, except for the fire test of methanol. Moreover, the fire alarm algorithms took much shorter times to alarm in cases where the smoke detector did alarm. For example, the fire test of toluene indicated that the smoke sensor detected the fire at 59 s, the fire alarm algorithm detected it at 56 s, and the fire was visually recorded at 50 s after the data acquisition started. In another example, the fire test of

green canvas indicated that the smoke sensor detected the fire at 1633 s, the fire alarm algorithm detected it at 1365 s, and the visual onset of fire was at 1395 s. Clearly, the fire alarm algorithm that incorporates both gas sensors and smoke detector alarmed at a time closer to the visual onset of the fire.

A fire alarm algorithm based on the detections of smoke, and CO or CO_2 concentrations will be sufficient for the heptane and toluene fires as shown in Figs. 5 and 6, since all three measured components rise at about the same time. However, for the fire test of HDPE in Fig. 7, a fire alarm algorithm must be based on the detections of smoke, CO and CO_2 concentrations in order to detect this fire on time. Certainly, a fire alarm algorithm based solely on the detections of smoke and CO_2 concentrations will detect the fire at a much later time after the visual onset of the fire, since CO_2 concentration rise at a much later time compared to smoke concentration. Moreover, the smoke sensor alarmed 316 s after the visual onset of fire.

Neither the fire alarm algorithms nor the smoke detector operating alone detected the methanol fire. No visible smoke was generated by this fire, so the smoke detector did not show any rise in voltage. Thus, the fire alarm algorithm based on first detecting a rate of increase of smoke exceeding a predetermined threshold rate and then checking the rates of increase of CO and CO_2 concentrations cannot detect this type of fire. That is, a fire alarm algorithm based on [CO_Alarm + SMOKE_Alarm = 2] or [CO2_Alarm + SMOKE_Alarm = 2] cannot detect the methanol fire. Note that [CO_Alarm = 1] indicates that the rate of increase of CO concentration has exceeded its predetermined threshold rate, and [CO_Alarm = 0] means the threshold rate has not been exceeded. However, the time traces of CO and CO_2 concentrations do indicate sharp rises. By modifying the fire alarm algorithm to be [CO_Alarm + CO2_Alarm + SMOKE_Alarm $\geq$ 2], the methanol

fire was actually detected at 248 s; that is 51 s after the visual indication of a fire (*t* = 197 s). An algorithm based on based on CO and CO_2, that is [CO_Alarm + CO2_Alarm = 2], will alarm promptly for the cases of Heptane and Toluene in which concentrations of CO and CO_2 rise at about the same time, but not for smoldering fires (e.g. HDPE).

4.4 Effects of nuisances on fire alarm algorithm

The effects of possible nuisances found in cargo compartments were used to assess the robustness of the fire alarm algorithm. The nuisances included dry ice, insecticide bomb, halon, and vapors of water, methanol, ethanol, acetone, and ammonia.

Insecticide *bomb*, which uses an aerosol to dispense a thick cloud of insecticide, is routinely used in aircraft cargo compartments on certain overseas flight to avoid spreading agricultural pests. The bomb caused a large signal on the smoke detector, but no noticeable rise in the CO and CO_2 signals. On the contrary, dry ice generated a rise in the CO_2 signal, but no rise in the smoke or CO signals. These nuisance sources caused no false alarm. However, the combination of dry ice and insecticide could potentially generate a false alarm. The intentional release of an insecticide bomb in flight is an unlikely scenario, but dry ice will be present in most flights for refrigeration purposes.

Of all the vapors tested, a small interference between methanol and CO_2 was observed. High methanol concentrations could make the instrument susceptible to false alarms, but this may reduce the real hazards associated with high concentrations of this flammable vapor. In a scenario where methanol, ethanol, and acetone vapors are high enough to trigger the smoke detector, and a fire is occurring at the same time, the

algorithm would have detected the fire since CO_2 concentrations would have risen due to the fire.

More significant is the observation that the laser through-put drops dramatically as a result of broad-band absorption by the halon mixture (halons 1301 and 1211). The decrease in transmitted laser through halon vapor is so severe that CO and CO_2 concentrations could not be measured. Because halon 1301 is used onboard aircraft to suppress fires, it will be present after a fire is detected and the agent is released. The ability of the fire sensor system to continue monitoring the cargo compartments after the release of extinguishing agents could be compromised.

For each of the nuisance sources tested, there was no interference with both smoke and trace gas. As a consequence, no false alarms were generated by any of these sources released alone. The fire detection system with the alarm algorithm is immune to these nuisance sources which could be found in-flight.

5. Summary

A fire sensor system based on the simultaneous detection CO, CO_2, and smoke concentrations, is demonstrated. The rates of increase of these three components are used in the fire alarm algorithm to determine the presence of a fire. The algorithm monitors the rate of increase of smoke level, and when this rate exceeds its threshold rate, the rates of increase of CO and CO_2 concentrations are checked. When either the rate of increase of CO or CO_2 concentration exceeds its threshold rate, a fire alarm is initiated. The fire detection system was found to perform better than a smoke detector operating alone. In cases where the smoke detector did not alarm, the algorithm was able detect the fire. However, in cases where the smoke detector did alarm, the

algorithm detected the fire in a much shorter time. The nuisance sources did not cause the fire detection system to generate false alarms.

An advantage of the fire alarm algorithm is that the signal to noise ratio for the temporal derivatives of measurements improves more rapidly with increasing time window length than does the signal to noise ratio for the mean of data points within the time window; this allows the alarm threshold to be set at a more sensitive value without causing noise-generated false alarm. A second advantage is that the alarm point is insensitive to constant offsets in the gas concentration measurements.

Although, the fire detection system was originally conceived to be deployed in cargo compartments of aircraft, it can also be applied to buildings, ship compartments, submarines, living compartments in space, and concealed cavities used for running electrical wires and plumbing. Future work will focus on the improvement of the minimum detection of CO and CO_2 concentrations by using separate lasers for each chemical species, and selecting stronger absorption lines where these two chemical species do not overlap.

Acknowledgments

This research is supported by NASA Small Business Innovative Research (SBIR) program under contract NAS3-01125, with Robert Anderson of NASA Glenn Research Center as the technical monitor.

Table 1: Fire Alarm Algorithm Performance

Case	*Material*	*Ignition Method*	*Fire Type*	*Visual [s]*	*Smoke [s]*	*Method A [s]*	*Method B* [s]
1	Heptane	Lighter	Flaming	218	N/A	242	243
2	Toluene	Lighter	Flaming	50	59	56	52
3	Methanol	Lighter	Flaming	197	N/A	N/A	N/A
4	HDPE Beads	Lighter	Smoldering	310	616	320	327
5	PVC Clad Wire	Pilot	Smoldering	347	N/A	380	385
6	Mixed Plastics	Coil + Pilot	Flaming	310	474	322	328
7	Mixed Fabrics	Coil + Pilot	Smoldering	310	N/A	305	309
8	Mixed Fabrics	Coil	Smoldering	348	439	336	341
9	Green Canvas	Coil	Smoldering	1395	1633	1365	1469
10	Dry Ice	N/A	N/A	N/A	N/A	N/A	N/A

References

[1] Blake, D. (2000), Aircraft Cargo Compartment Smoke Detector Alarm Incidents on U.S.-Registered Aircraft, 1974-1999, DOT/FAA/AR-TN00/29.

[2] Blagojevich M., Petkovich D., and Simich, D. (2001), New Algorithm for Adaptive Alarm Threshold in Fire Detection System, 12th International Conference on Automatic Fire Detection.

[3] Milke, J. A. (1999), Using Multiple Sensors for Discriminating Fire Detection, *Fire Technol.* **35**:195-209.

[4] Gottuk D. T., Peatross M. J., Roby, R. J., and Beyler, C. L. (2002), Advanced Fire Detection Using Multi-Signature Alarm Algorithms, Fire Safety Journal 37:381-394.

[5] Marman, D. H, Peltier, M. A., and Wong, J. Y. (1999), Fire and Smoke Detection and Control System, US Patent No. 5,945,924.

[6] Rose-Pehrsson, S. L., Hart, S. J., Street, T. T., Tatem, P. A., Williams, F., Hammond, M. H, Gottuk, D. T., Wright, M. T. and Wong, J. Y. (2001), Real-Time Probabilistic Neural Network Performance and Optimization for Fired Detection and Nuisance Alarm Rejection, 12th International Conference on Automatic Fire Detection.

[7] Herriott, D.R., et al. (1964), Off-Axis Paths in Spherical Mirror Interferometers, *Appl. Opt*.**3:**523-526.

[8] Rothmann, L.S., Gamache, R.R., et al. (2001), *J. Quant. Spectrosc. Radiat. Transfer* **48**:469.

[9] Silver, J.A. (1992), Frequency Modulation Spectroscopy for Trace Species Detection: Theory and Comparison, *Appl. Opt.* **31**:707-717.

[10] Bomse, D.S., et al. (1992), Frequency Modulation Spectroscopy for Trace Species

Detection: Experimental Comparison of Methods, *Appl. Opt.*, vol. **31**, 718-731.

[11] Chen, S.-J. (2006), Fire Alarm Algorithm Using Smoke and Gas Sensors, U.S. Patent No. 7,142,105.

Legends to Illustrations

Figure 1. Schematic of the fire testing facility.

Figure 2. Schematic of optical setup for diode laser-based detection of carbon dioxide and carbon monoxide.

Figure 3. Absorption lines of CO and CO_2 calculated from HITRAN database.

Figure 4. Decision tree of fire alarm algorithm. ROI denotes rate of increase.

Figure 5. Heptane combustion. Time histories of CO, CO_2, smoke, and fire status.

Figure 6. Toluene combustion. Time histories of CO, CO_2, smoke, and fire status.

Figure 7. HDPE beads combustion. Time histories of CO, CO_2, smoke, and fire status.

Figure 8. Moving-averaged time histories of CO (*a*) and CO_2 (*b*). Traces are offset for clarity. Bottom to top: time window of 1, 5, 10, 15, and 20 s. Longer windows reduce noise but introduce a delay in the response, most notable at the CO peak in Fig. 8a.

Figure 9. Standard deviations versus time window of moving-average for CO (*a*) and CO_2 (*b*)

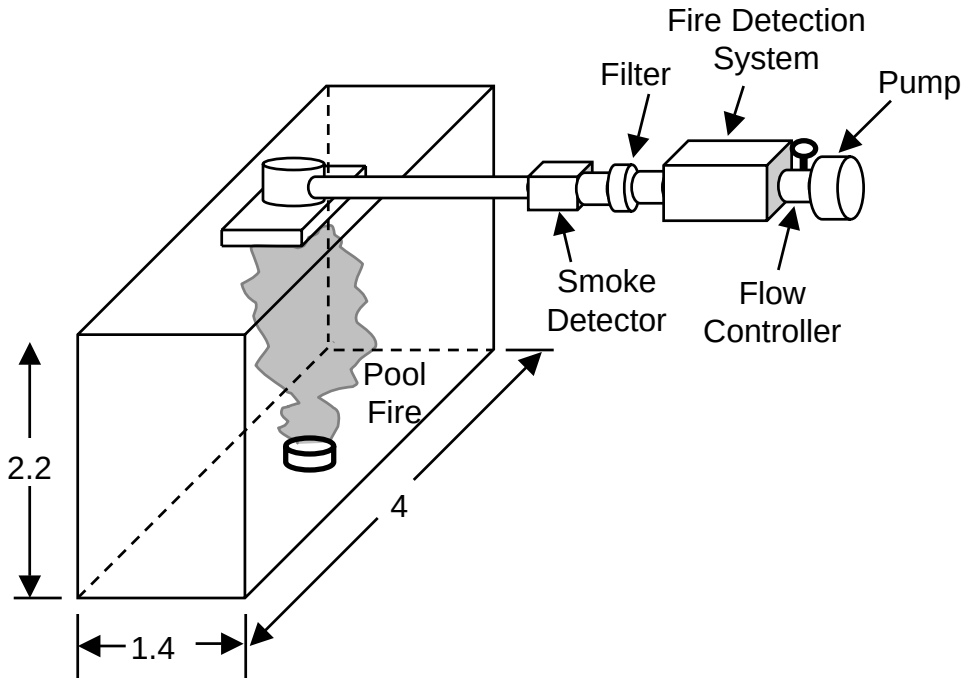
Fire Detection
System
Filter
Pump
Smoke
Detector
Flow
Controller
Pool
Fire
2.2
4
1.4

FIGURE 1

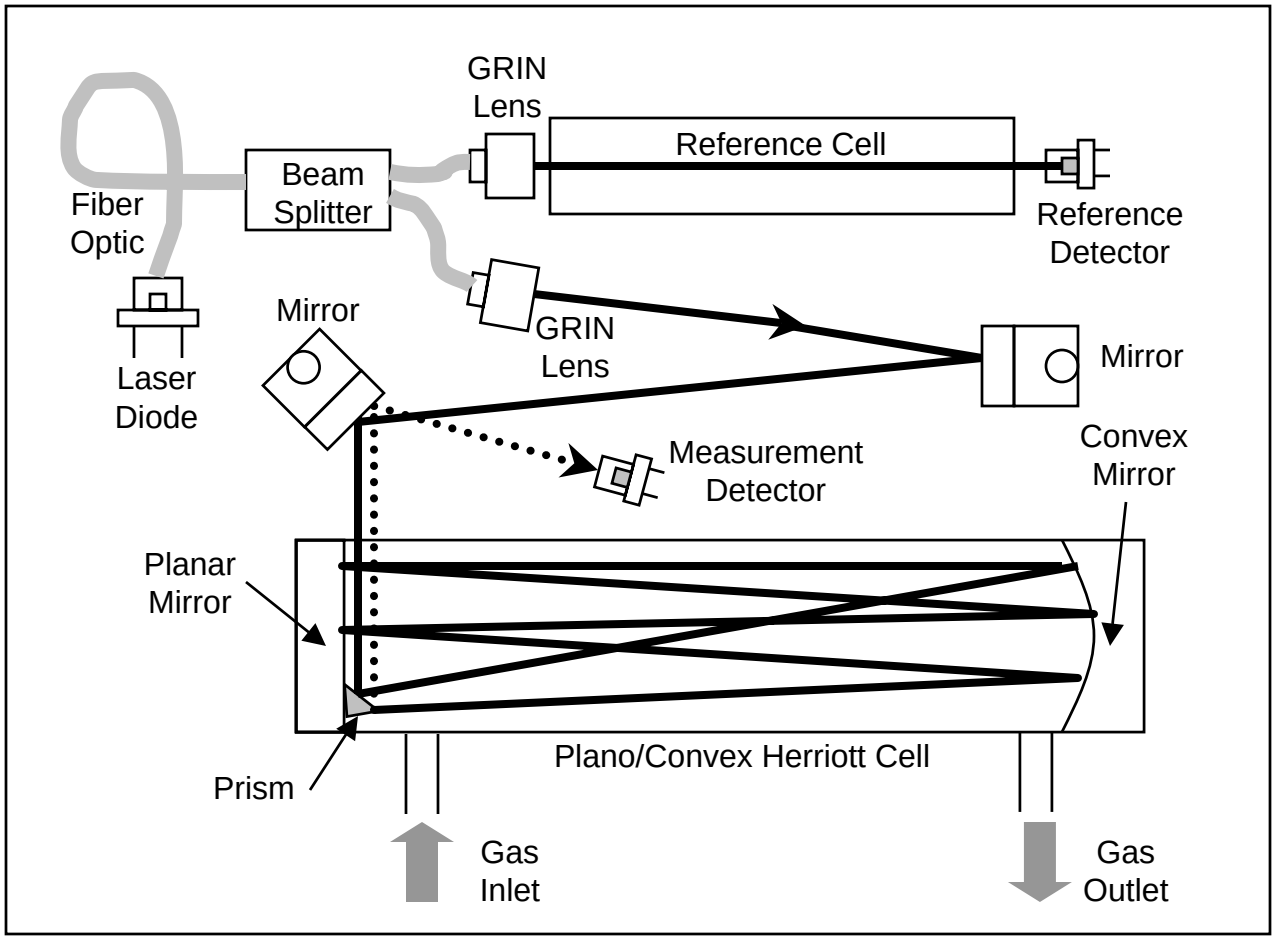
GRIN
Lens
Reference Cell
Beam
Splitter
Fiber
Optic
Reference
Detector
Mirror
GRIN
Lens
Mirror
Laser
Diode
Measurement
Detector
Convex
Mirror
Planar
Mirror
Plano/Convex Herriott Cell
Prism
Gas
Inlet
Gas
Outlet

FIGURE 2

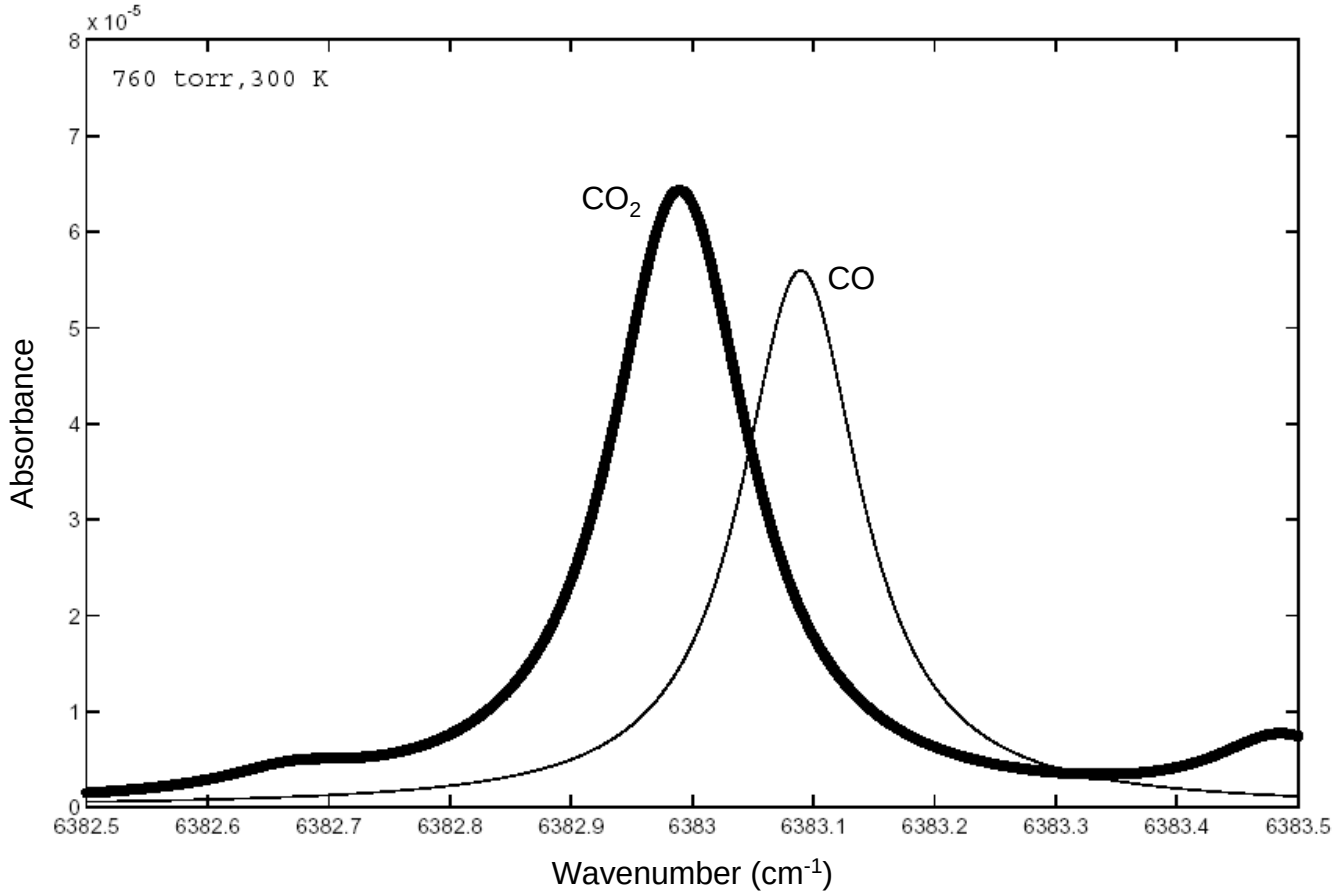
x 10-5
760 torr,300 K
CO2
CO
Absorbance
Wavenumber (cm-1)
0
1
2
3
4
5
6
7
8
6382.5
6382.6
6382.7
6382.8
6382.9
6383
6383.1
6383.2
6383.3
6383.4
6383.5

FIGURE 3

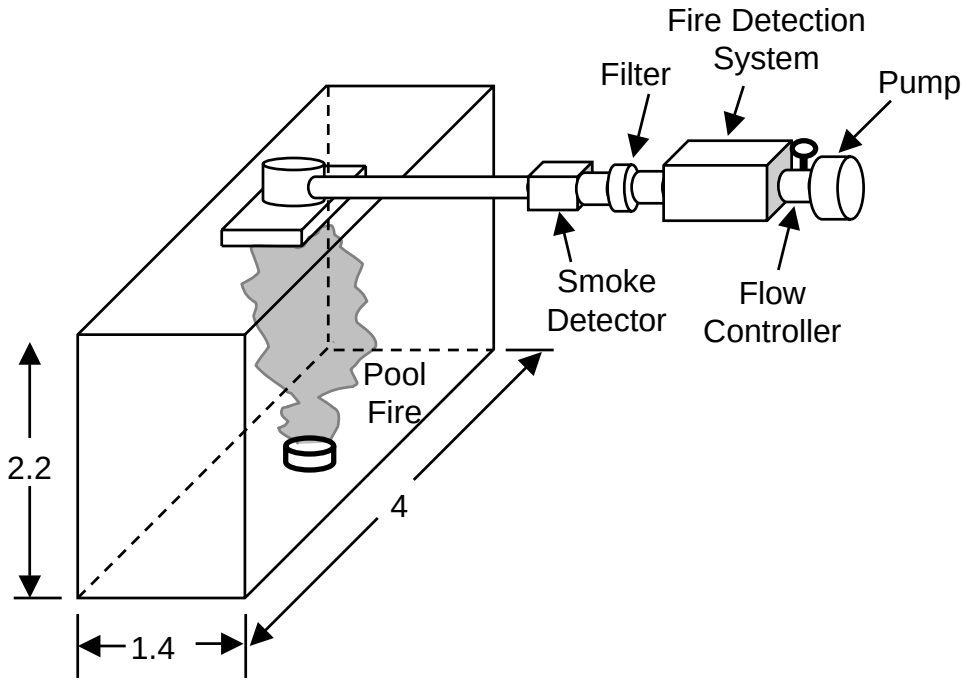
Fire Detection
System
Filter
Pump
Smoke
Detector
Flow
Controller
Pool
Fire
2.2
4
1.4

FIGURE 3

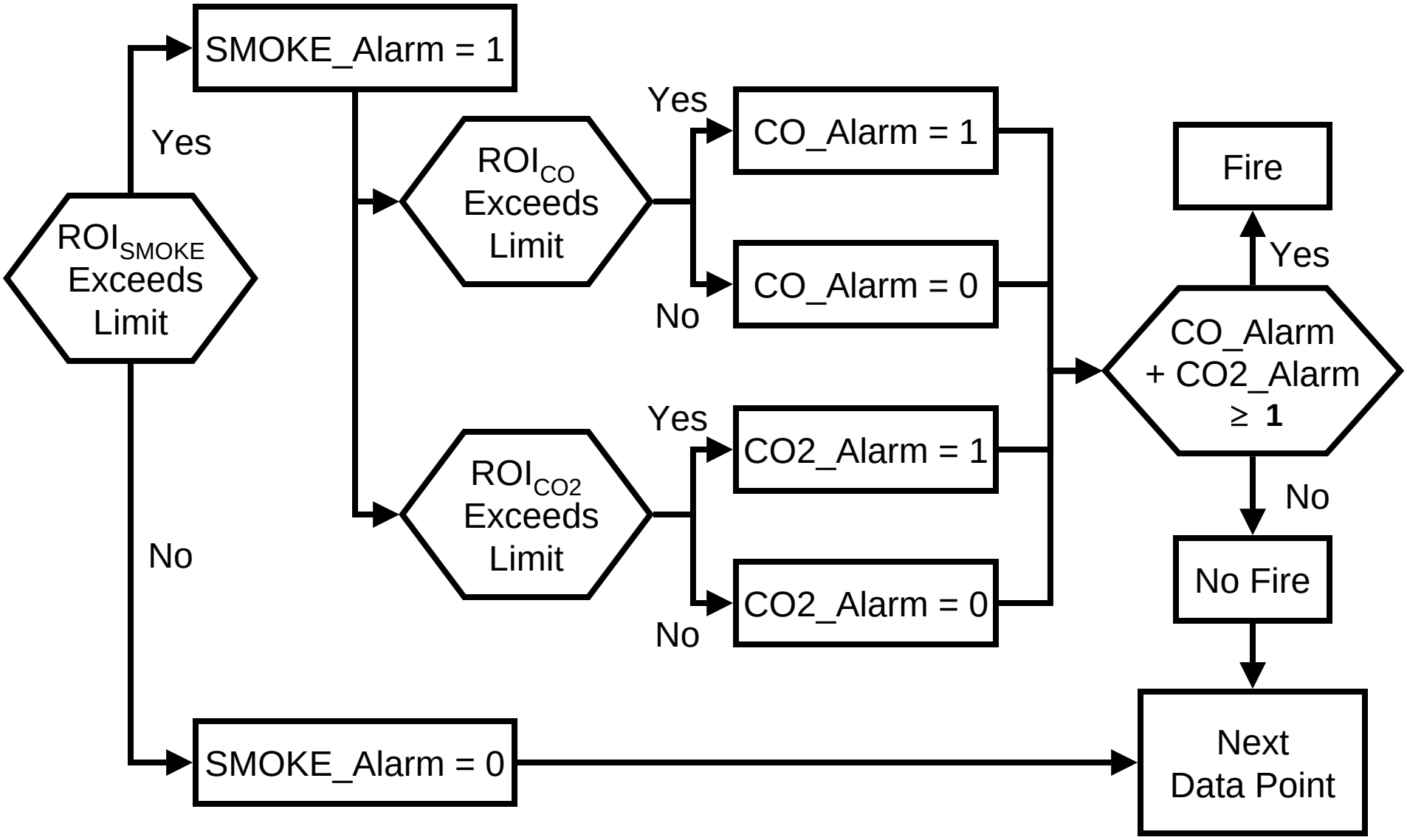
SMOKE_Alarm = 1
Yes
ROI$_{SMOKE}$ Exceeds Limit
No
ROI$_{CO}$ Exceeds Limit
Yes
CO_Alarm = 1
No
CO_Alarm = 0
ROI$_{CO2}$ Exceeds Limit
Yes
CO2_Alarm = 1
No
CO2_Alarm = 0
CO_Alarm + CO2_Alarm ≥ 1
Yes
Fire
No
No Fire
SMOKE_Alarm = 0
Next Data Point

FIGURE 4

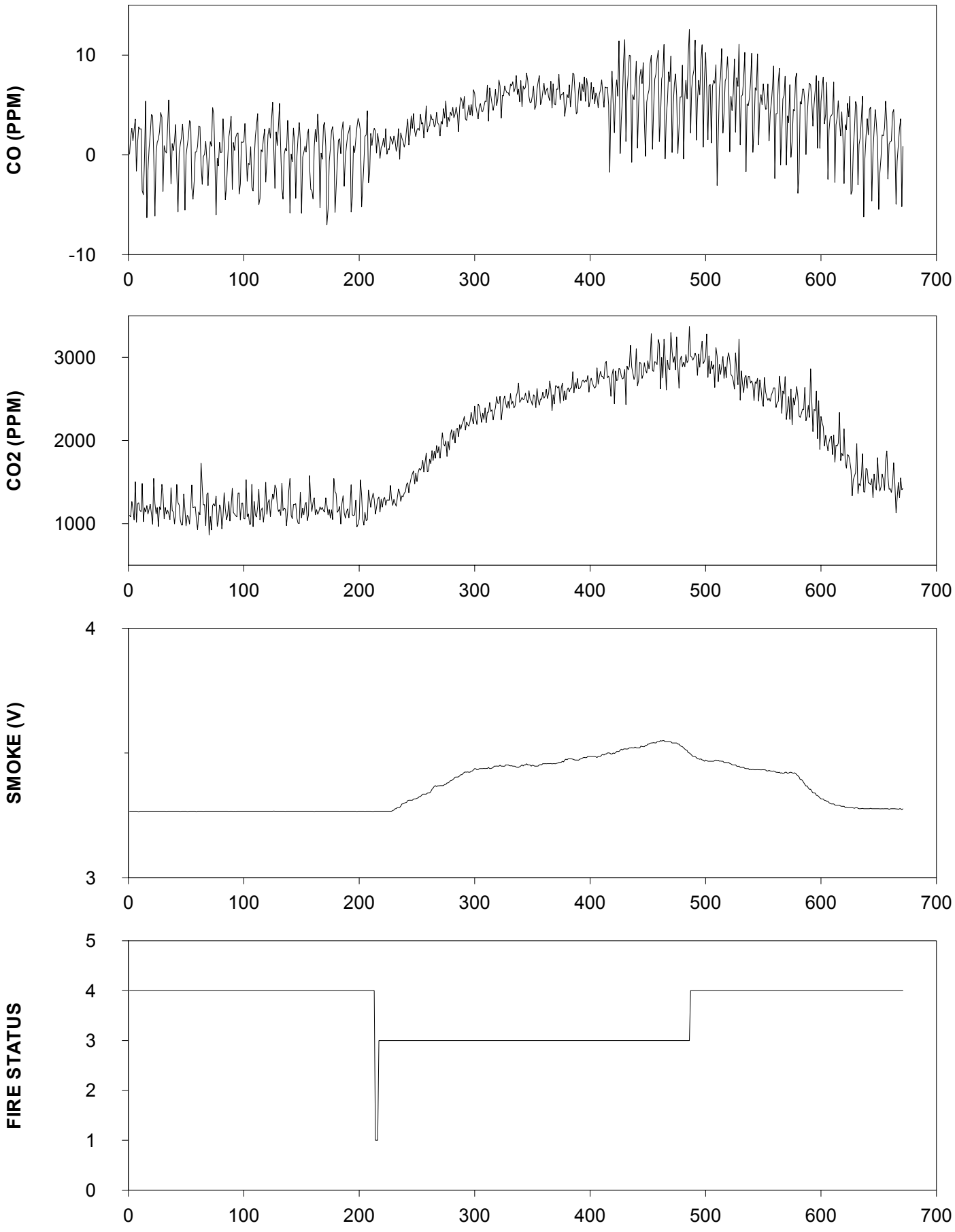
CO (PPM)
10
0
-10
0
100
200
300
400
500
600
700
CO2 (PPM)
3000
2000
1000
SMOKE (V)
4
3
FIRE STATUS
5
4
3
2
1
0
HEPTANE
Elapsed Time [s]

FIGURE 5

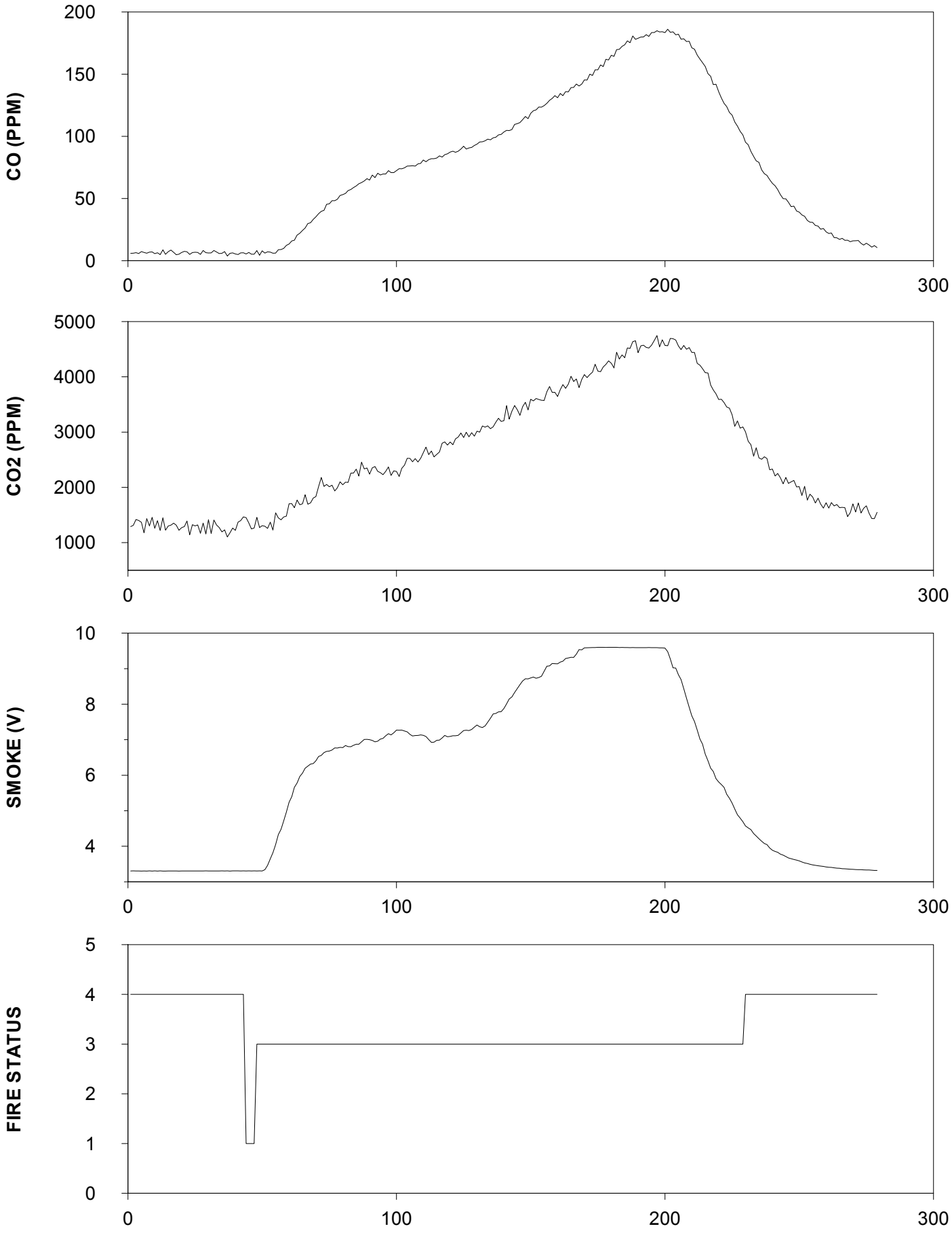
CO (PPM)
200
150
100
50
0
0
100
200
300
CO2 (PPM)
5000
4000
3000
2000
1000
0
100
200
300
SMOKE (V)
10
8
6
4
0
100
200
300
FIRE STATUS
5
4
3
2
1
0
0
100
200
300
TOLUENE
Elapsed Time [s]

FIGURE 6

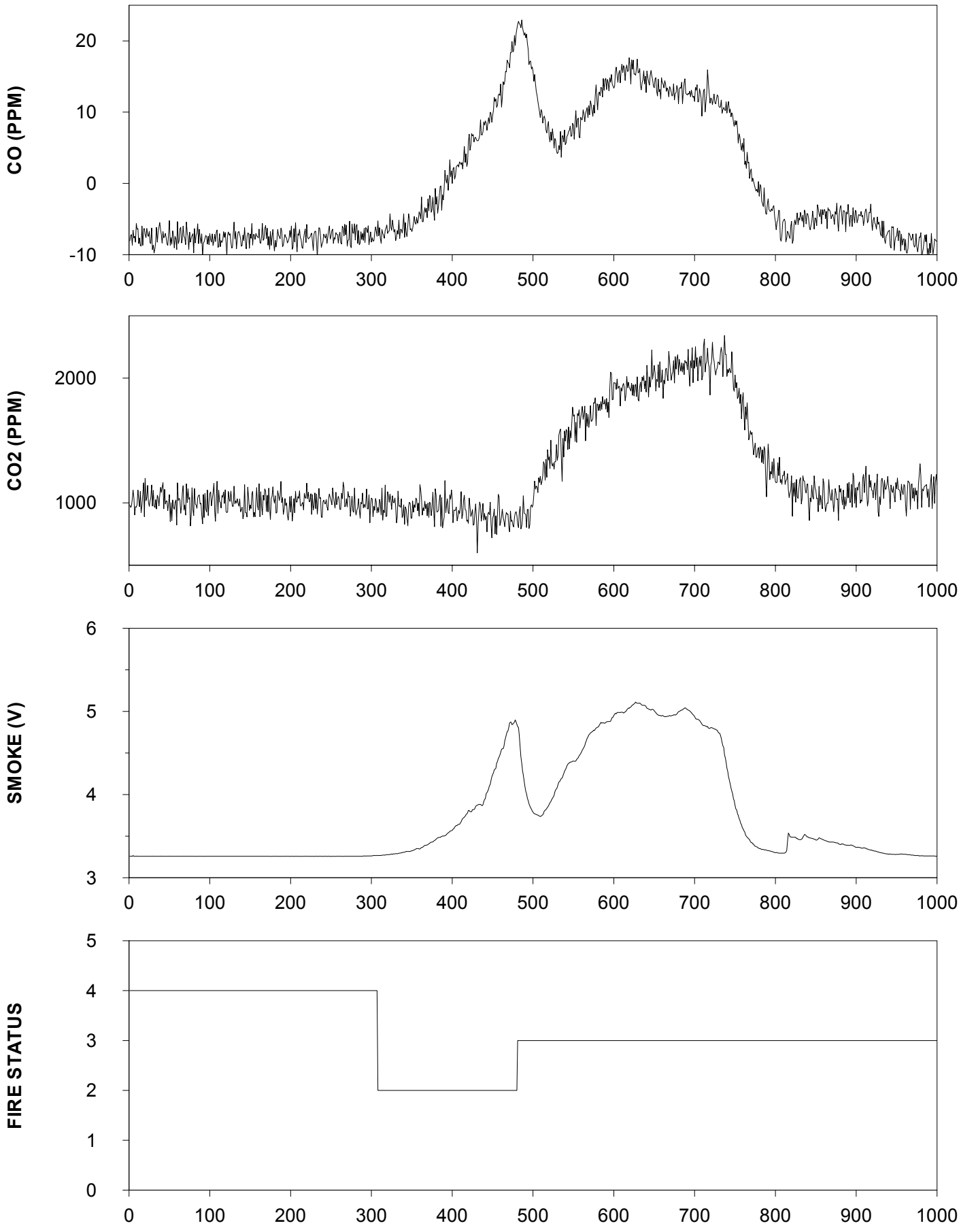
CO (PPM)
20
10
0
-10
0
100
200
300
400
500
600
700
800
900
1000
CO2 (PPM)
2000
1000
SMOKE (V)
6
5
4
3
FIRE STATUS
5
4
3
2
1
0
HDPE
Elapsed Time [s]

FIGURE 7

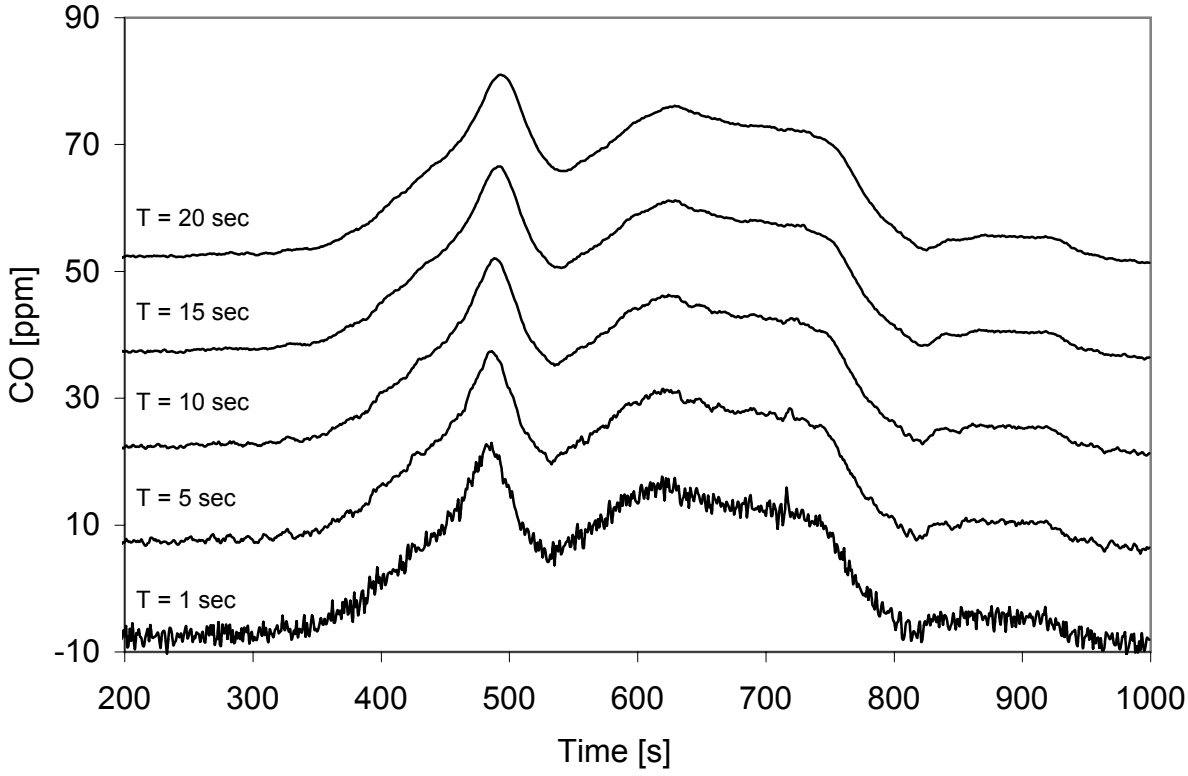
90
70
50
30
10
-10
CO [ppm]
T = 20 sec
T = 15 sec
T = 10 sec
T = 5 sec
T = 1 sec
200
300
400
500
600
700
800
900
1000
Time [s]

FIGURE 8a

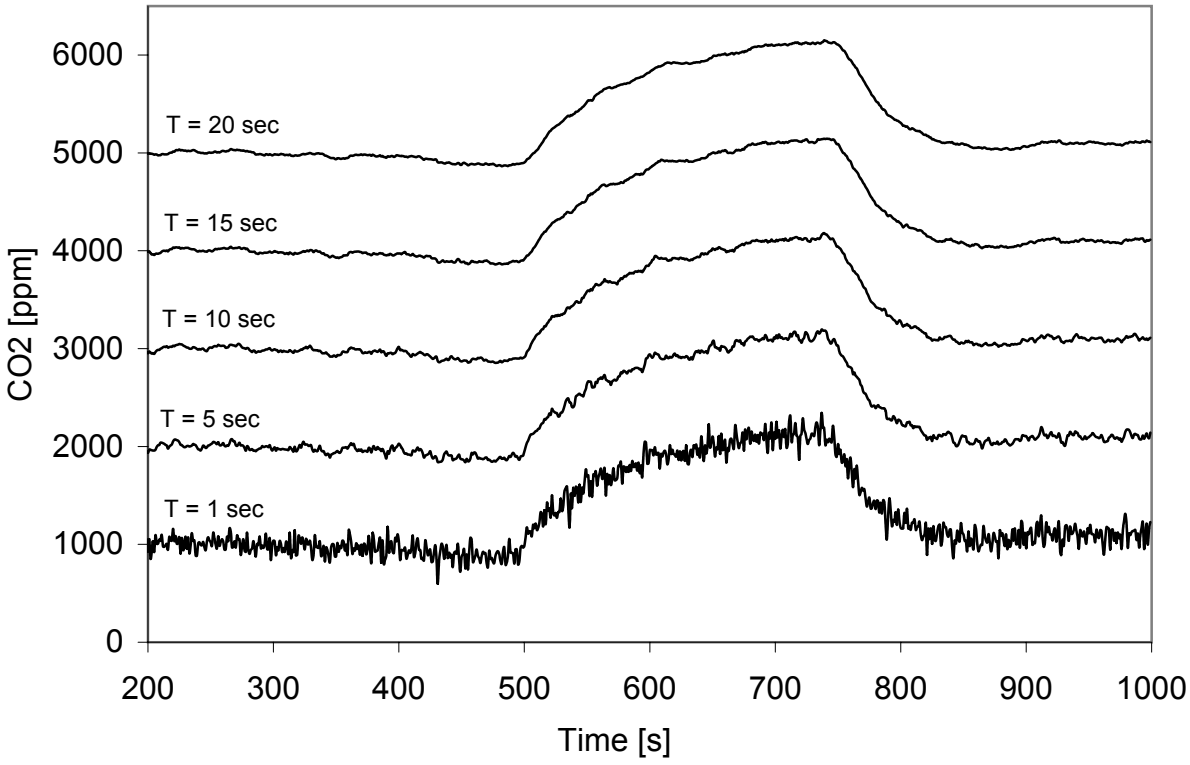
6000
5000
4000
3000
2000
1000
0
CO2 [ppm]
T = 20 sec
T = 15 sec
T = 10 sec
T = 5 sec
T = 1 sec
200
300
400
500
600
700
800
900
1000
Time [s]

FIGURE 8b

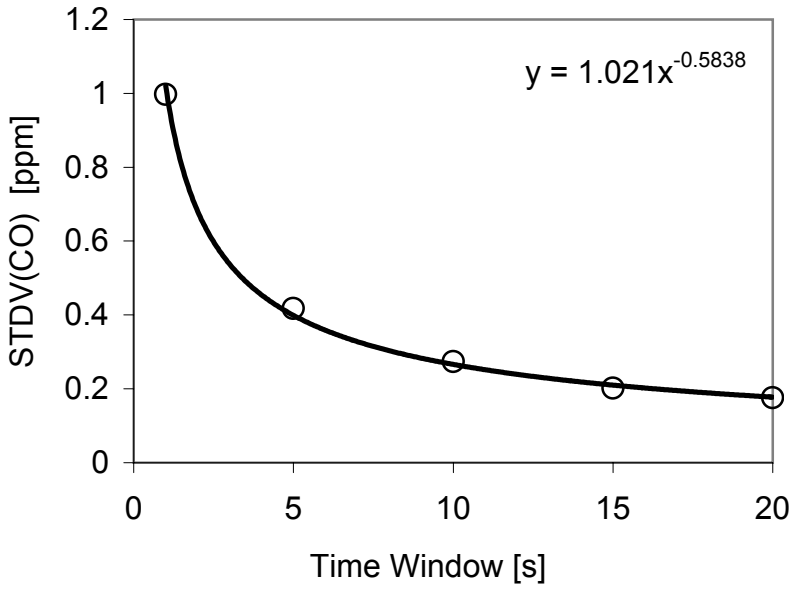
y = 1.021x^-0.5838
STDV(CO) [ppm]
Time Window [s]
1.2
1
0.8
0.6
0.4
0.2
0
0
5
10
15
20

FIGURE 9a

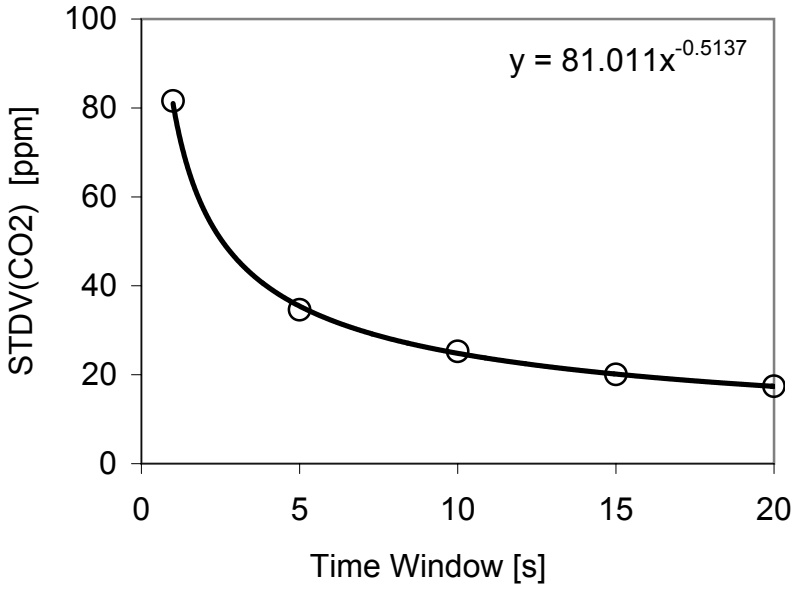
y = 81.011x^-0.5137
STDV(CO2) [ppm]
Time Window [s]
0
20
40
60
80
100
0
5
10
15
20

FIGURE 9b